THE JOURNAL OF PHYSICAL CHEMISTRY Letters

pubs.acs.org/JPCL Letter

Polarized Fock States and the Dynamical Casimir Effect in Molecular Cavity Quantum Electrodynamics

Arkajit Mandal,* Sebastian Montillo Vega, and Pengfei Huo*

Cite This: J. Phys. Chem. Lett. 2020, 11, 9215−9223 Read Online

ACCESS | Metrics & More | Article Recommendations | Supporting Information

ABSTRACT: We present a new theoretical framework, polarized Fock states (PFSs), to describe the coupled molecule−cavity hybrid system in quantum electrodynamics. Through the quantum light−matter interactions under the dipole Gauge, the molecular permanent dipoles polarize the photon field by displacing the photonic coordinate. Hence, it is convenient to use these shifted Fock states (termed the PFSs) to describe light−matter interactions under the strong coupling regimes. These PFSs are nonorthogonal to each other and are light−matter entangled states. They allow an intuitive understanding of several phenomena that go beyond the prediction of the quantum Rabi model, while also offering numerical convenience to converge the results with much fewer states. With this powerful new theoretical framework, we explain how molecular permanent dipoles lead to the generation of multiple photons from a single electronic excitation (down-conversion), effectively achieving the dynamical Casimir effect through the nuclear vibration instead of cavity mirror oscillations.

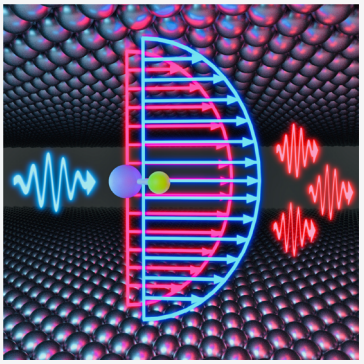

Coupling molecular systems to an optical cavity can significantly alter their potential energy landscape[1−4] and enable new chemical reactivities beyond the existing paradigms of chemistry. The existing theoretical framework for describing such a molecule−cavity hybrid system is based upon adiabatic electronic states for the molecular subsystem and the Fock states for the quantized radiation mode inside the cavity.[5−19] While the adiabatic-Fock state is commonly used for describing matter−cavity interactions,[20,21] it might not be the most convenient representation for describing strong interactions between the matter and the cavity.[22−27] In this work, we present a new representation based on the idea of the polarized Fock states, which allows one to intuitively understand new phenomena that go beyond the prediction of the quantum Rabi model.

In particular, this new representation serves as a convenient tool to analyze the role of molecular permanent dipoles in polariton chemistry. We note that there are existing works to understand the role of the permanent dipole in the light−matter interactions between few-level matter systems and radiation.[28−34] However, the role of the permanent dipole as well as the associated dipole self-energies in the emerging field of polaritonic chemistry remains to be clarified, despite recent works[11,12,35,36] that have considered these terms in the light−matter interaction.

We start by considering the Pauli−Fierz (PF) nonrelativistic QED Hamiltonian[16,23,37] to describe the light−matter interaction. The PF Hamiltonian can be rigorously derived[12,23,38] (see the Supporting Information for details) by applying the Power−Zienau−Woolley (PZW) Gauge transformation[39,40] and a unitary phase transformation[38] on the minimal-coupling Hamiltonian in the Coulomb gauge (i.e., the "p·A" Hamiltonian) under the long-wavelength limit. For a molecule coupled to a single photon mode inside an optical cavity, the PF Hamiltonian is

$$\begin{aligned}\hat{H}_{\mathrm{PF}} &= \hat{H}_{\mathrm{M}} + \frac{1}{2}\hat{p}^2 + \frac{1}{2}\omega_{\mathrm{c}}^2\left(\hat{q} + \sqrt{\frac{2}{\hbar\omega_{\mathrm{c}}^3}}\boldsymbol{\chi}\cdot\hat{\boldsymbol{\mu}}\right)^2 \\ &= \hat{H}_{\mathrm{M}} + \left(\hat{a}^\dagger\hat{a} + \frac{1}{2}\right)\hbar\omega_{\mathrm{c}} + \boldsymbol{\chi}\cdot\hat{\boldsymbol{\mu}}(\hat{a}^\dagger + \hat{a}) + \frac{(\boldsymbol{\chi}\cdot\hat{\boldsymbol{\mu}})^2}{\hbar\omega_{\mathrm{c}}}\end{aligned} \tag{1}$$

In the last line of eq 1, $\hat{H}_{\mathrm{M}}$ represents the molecular Hamiltonian; the second term $\hat{H}_{\mathrm{ph}} = \left(\hat{a}^\dagger\hat{a} + \frac{1}{2}\right)\hbar\omega_{\mathrm{c}}$ represents the Hamiltonian of the vacuum photon field inside the cavity with the frequency ω_{c}; the third term describes the light−matter interaction in the electric-dipole "d·E" form,[40] with $\boldsymbol{\chi} = \sqrt{\frac{\hbar\omega_{\mathrm{c}}}{2\varepsilon_0\mathcal{V}}}\hat{\mathbf{e}} \equiv \chi\hat{\mathbf{e}}$ characterizing the light−matter coupling vector oriented in the direction of polarization unit vector $\hat{\mathbf{e}}$, $\mathcal{V}$ as the quantization volume for the photon field, and ε_0 as the permittivity inside the cavity. The last term is the dipole self-energy (DSE), which describes how the polarization of the matter acts back on the photon field.[9] Further, $\hat{a}^\dagger$ and $\hat{a}$

Received: August 5, 2020
Accepted: September 29, 2020
Published: September 29, 2020

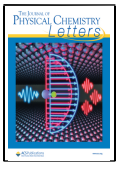

are the photon creation and annihilation operator; $\hat{q} = \sqrt{\hbar/2\omega_c}(\hat{a}^\dagger + \hat{a})$ and $\hat{p} = i\sqrt{\hbar\omega_c/2}(\hat{a}^\dagger - \hat{a})$ are the photonic coordinate and momentum operator, respectively; and $\hat{\mu}$ is the molecular dipole operator (for both electrons and nuclei). Throughout this study, we assume that $\hat{e}$ aligns with the direction of $\hat{\mu}$.

The matter Hamiltonian is expressed as

$$\hat{H}_M = \hat{T}_{\mathbf{R}} + \hat{H}_{el}(\mathbf{R}, \mathbf{r}) \tag{2}$$

where $\hat{T}_{\mathbf{R}} = \hat{P}^2/2\mathbf{M} = -\hbar^2\nabla_{\mathbf{R}}^2/2\mathbf{M}$ is the nuclear kinetic energy operator and $\hat{H}_{el}(\mathbf{r}, \mathbf{R}) = \hat{T}_r + \hat{V}_{coul}(\mathbf{R}, \mathbf{r})$ is the electronic Hamiltonian, with the electronic kinetic energy $\hat{T}_{\mathbf{r}}$ and Coulomb potential $\hat{V}_{coul}(\mathbf{R}, \mathbf{r})$ among electrons and nuclei. The electronic adiabatic state $|\psi_i(\mathbf{R})\rangle$ is defined as the eigenstate of $\hat{H}_{el}$ as follows

$$\hat{H}_{el}|\psi_i(\mathbf{R})\rangle = E_i(\mathbf{R})|\psi_i(\mathbf{R})\rangle \tag{3}$$

In the adiabatic electronic subspace $\{|\psi_i(\mathbf{R})\rangle\}$, the matter Hamiltonian can be expressed as[41,42]

$$\hat{H}_M = \frac{1}{2\mathbf{M}}\left(\hat{P} - i\hbar\sum_{ij}\mathbf{d}_{ij}|i\rangle\langle j|\right)^2 + \sum_i E_i(\mathbf{R})|i\rangle\langle i| \tag{4}$$

where we have used the shorthand notation $|i\rangle \equiv |\psi_i(\mathbf{R})\rangle$ and $\mathbf{d}_{ij} = \langle \psi_i(\mathbf{R})|\nabla_{\mathbf{R}}\psi_j(\mathbf{R})\rangle$ is the derivative coupling. Note that the above equation is equivalent[41,42] to the commonly used form of the vibronic Hamiltonian $\hat{H}_M = -\frac{\hbar^2}{2\mathbf{M}}\sum_{ij}[\nabla_{\mathbf{R}}^2\delta_{ij} + 2\mathbf{d}_{ij}\cdot\nabla_{\mathbf{R}} + \mathbf{D}_{ij}]|i\rangle\langle j| + \sum_i E_i(\mathbf{R})|i\rangle\langle i|$, where $\mathbf{D}_{ij} = \langle\psi_i(\mathbf{R})|\nabla_R^2\psi_j(\mathbf{R})\rangle$ is the second-derivative coupling. A simple proof is provided in the Supporting Information.

The polaritonic Hamiltonian is defined[9,43] as $\hat{H}_{pl} \equiv \hat{H}_{PF} - \hat{T}_R$, with the following eigenequation

$$\hat{H}_{pl}|\Phi_j(\mathbf{R})\rangle \equiv (\hat{H}_{PF} - \hat{T}_R)|\Phi_j(\mathbf{R})\rangle = \mathcal{E}_j(\mathbf{R})|\Phi_j(\mathbf{R})\rangle \tag{5}$$

The polariton surface $\mathcal{E}_j(\mathbf{R})$ and polariton state $|\Phi_j(\mathbf{R})\rangle$ are the eigenvalue and eigenstate of $\hat{H}_{pl}$.To solve it, one often makes an explicit truncation of the electronic subspace $\{|\psi_i\rangle\}$ by considering only two electronic states $\{|g(\mathbf{R})\rangle, |e(\mathbf{R})\rangle\}$ (or a few electronic states[44]), while trying to approach to the complete basis limit for the photonic DOF. The reason behind this truncation is that usually only a few low-lying electronic states that are accessible will play a role in the polaritonic dynamics. In fact, a few-level electronic truncation often provides accurate results when using the "d·E" form.[45−47] This is advantageous because it is very difficult to obtain accurate excited electronic states for the matter Hamiltonian. The commonly used representation to solve the above eigenequation is the adiabatic-Fock basis, $\{|g(\mathbf{R})\rangle \otimes |n\rangle, |e(\mathbf{R})\rangle \otimes |n\rangle\}$, with eigenstates of the electronic Hamiltonian $\hat{H}_{el}$, i.e., the adiabatic electronic states $\{|g(\mathbf{R})\rangle, |e(\mathbf{R})\rangle\}$ for the matter part, and the Fock states of the radiation mode (vacuum photon field) $\{|n\rangle\}$, i.e., the eigenstate of $\left(\hat{a}^\dagger\hat{a} + \frac{1}{2}\right)\hbar\omega_c$.

For an atom, $\hat{H}_M = E_g|g\rangle\langle g| + E_e|e\rangle\langle e|$, and the transition dipole is $\boldsymbol{\mu}_{eg} = \langle e|\hat{\mu}|g\rangle$. Note that the permanent dipoles are $\boldsymbol{\mu}_{ee} = \langle e|\hat{\mu}|e\rangle = 0$, $\boldsymbol{\mu}_{gg} = \langle g|\hat{\mu}|g\rangle = 0$. Thus, the dipole operator is expressed as $\hat{\mu} = \boldsymbol{\mu}_{eg}(|e\rangle\langle g| + |g\rangle\langle e|) \equiv \mu_{eg}(\hat{\sigma}^\dagger + \hat{\sigma})$ by defining the creation operator $\hat{\sigma}^\dagger \equiv |e\rangle\langle g|$ and annihilation operator $\hat{\sigma} \equiv |g\rangle\langle e|$ of the electronic excitation. The atom−cavity PF Hamiltonian becomes $\hat{H}_{PF} = \hat{H}_M + \hat{H}_{ph} + \boldsymbol{\chi}\cdot\boldsymbol{\mu}_{eg}(\hat{\sigma}^\dagger + \hat{\sigma})(\hat{a}^\dagger + \hat{a}) + \frac{(\boldsymbol{\chi}\cdot\boldsymbol{\mu}_{eg})^2}{\hbar\omega_c}$. Dropping the DSE (the last term) leads to the Rabi model[48]

$$\hat{H}_{Rabi} = \hat{H}_M + \hat{H}_{ph} + \boldsymbol{\chi}\cdot\boldsymbol{\mu}_{eg}(\hat{\sigma}^\dagger + \hat{\sigma})(\hat{a}^\dagger + \hat{a}) \tag{6}$$

Further dropping the counter-rotating terms $\hat{\sigma}^\dagger\hat{a}^\dagger$ and $\hat{\sigma}\hat{a}$ leads to the well-known Jaynes−Cummings model[20] $\hat{H}_{JC} = \hat{H}_M + \hat{H}_{ph} + \boldsymbol{\chi}\cdot\boldsymbol{\mu}_{eg}(\hat{\sigma}^\dagger\hat{a} + \hat{\sigma}\hat{a}^\dagger)$.

For a molecule under the truncated electronic subspace $\{|g(\mathbf{R})\rangle, |e(\mathbf{R})\rangle\}$, the molecular Hamiltonian is $\hat{H}_M = \frac{1}{2M}\left(\hat{P} - i\hbar\sum_{ij\in g,e}\mathbf{d}_{ij}|i(\mathbf{R})\rangle\langle j(\mathbf{R})|\right)^2 + E_g(\mathbf{R})|g(\mathbf{R})\rangle\langle g(\mathbf{R})| + E_e(\mathbf{R})|e(\mathbf{R})\rangle\langle e(\mathbf{R})|$. The dipole operator in this electronic subspace has the following expression

$$\begin{aligned}\hat{\mu} = {} & \boldsymbol{\mu}_{gg}(\mathbf{R})|g(\mathbf{R})\rangle\langle g(\mathbf{R})| + \boldsymbol{\mu}_{ee}(\mathbf{R})|e(\mathbf{R})\rangle\langle e(\mathbf{R})| \\ & + \boldsymbol{\mu}_{eg}(\mathbf{R})(|e(\mathbf{R})\rangle\langle g(\mathbf{R})| + |g(\mathbf{R})\rangle\langle e(\mathbf{R})|)\end{aligned} \tag{7}$$

where the adiabatic permanent dipoles are not necessarily zero. In the *same* truncated electronic subspace, we diagonalize eq 7 to obtain

$$\hat{\mu} = \boldsymbol{\mu}_I(\mathbf{R})|I\rangle\langle I| + \boldsymbol{\mu}_C(\mathbf{R})|C\rangle\langle C| = \sum_\alpha \boldsymbol{\mu}_\alpha(\mathbf{R})|\alpha\rangle\langle\alpha| \tag{8}$$

Here, $\alpha \in \{I, C\}$ are *eigenstates* of $\hat{\mu}$ in the *truncated electronic subspace*, which are denoted as the covalent state $|C\rangle$ and the ionic states $|I\rangle$ for a molecule in the truncated electronic subspace $\{|g(\mathbf{R})\rangle, |e(\mathbf{R})\rangle\}$. Note that $\{|C\rangle, |I\rangle\}$ are termed the Mulliken−Hush diabatic states[49−53] and are commonly used as approximate *diabatic* states that are defined based on their characters (covalent and ionic). In this work, we explicitly assume that $|I\rangle$ and $|C\rangle$ are strict diabatic states, hence $\langle C|\nabla_{\mathbf{R}}|I\rangle = 0$ (they are **R**-independent). This assumption simplifies our argument, but will not impact any conclusion we draw (see the Supporting Information for details). Note that there is no transition dipole in the diabatic representation ($\boldsymbol{\mu}_{IC} = 0$). For a special case of the atomic cavity QED where $\boldsymbol{\mu}_{ee} = \boldsymbol{\mu}_{gg} = 0$, $\hat{\boldsymbol{\mu}} = \boldsymbol{\mu}_{eg}|+\rangle\langle +| - \boldsymbol{\mu}_{eg}|-\rangle\langle -|$ and $|\pm\rangle = [|g\rangle \pm |e\rangle]/\sqrt{2}$ (the eigenstates of $\hat{\boldsymbol{\mu}}$) are referred to as the qubit states,[24,25,54,55] and the atomic Hamiltonian is $\hat{H}_M = \frac{\Delta}{2}[|+\rangle\langle -| + |-\rangle\langle +|]$, where $\Delta = E_e - E_g$, with the eigenvalue $\boldsymbol{\mu}_\pm = \pm\boldsymbol{\mu}_{eg}$.

With the MH diabatic states, the molecular Hamiltonian becomes

$$\hat{H}_M = \hat{T}_{\mathbf{R}} + \sum_\alpha V_\alpha(\mathbf{R})|\alpha\rangle\langle\alpha| + V_{IC}(\mathbf{R})(|c\rangle\langle I| + |I\rangle\langle c|) \tag{9}$$

where $V_\alpha(\mathbf{R})$ represents the diabatic potentials, $V_{IC}(\mathbf{R})$ represents the diabatic coupling. The PF Hamiltonian in eq 1 under the $|\alpha\rangle$ is expressed as

$$\hat{H}_{PF} = \hat{H}_M + \frac{\hat{p}^2}{2} + \sum_\alpha \frac{\omega_c^2}{2}(\hat{q} + q_\alpha^0(\mathbf{R})|\alpha\rangle\langle\alpha|)^2 \tag{10}$$

https://dx.doi.org/10.1021/acs.jpclett.0c02399
J. Phys. Chem. Lett. 2020, 11, 9215−9223

where $q_\alpha^0(\mathbf{R}) = \sqrt{\frac{2}{\hbar\omega_c^3}}\boldsymbol{\chi}\cdot\boldsymbol{\mu}_i(\mathbf{R})$. We notice that the photon field is described as displaced Harmonic oscillator that is centered around $-q_\alpha^0(\mathbf{R})$. This displacement can be viewed as a *polarization* of the photon field due to the presence of the molecule-cavity coupling, such that the photon field corresponds to a nonzero (hence polarized) vector potential, in contrast to the vacuum photon field.

The *central idea* of this work stems from the *polarized Fock states* (PFSs) defined as follows

$$\frac{1}{2}[\hat{p}^2 + \omega_c^2(\hat{q} + q_\alpha^0(\mathbf{R}))^2]|n_\alpha(\mathbf{R})\rangle \equiv \left(\hat{b}_\alpha^\dagger\hat{b}_\alpha + \frac{1}{2}\right)\hbar\omega_c|n_\alpha(\mathbf{R})\rangle = \left(n_\alpha + \frac{1}{2}\right)\hbar\omega_c|n_\alpha(\mathbf{R})\rangle \tag{11}$$

where the PFS $|n_\alpha(\mathbf{R})\rangle \equiv |n_\alpha\rangle$ is the Fock state of a displaced Harmonic oscillator, with the displacement $-q_\alpha^0 = -\sqrt{\frac{2}{\hbar\omega_c^3}}\boldsymbol{\chi}\cdot\boldsymbol{\mu}_\alpha(\mathbf{R})$ specific to the diabatic state $|\alpha\rangle$ such that $|n_\alpha\rangle = e^{-i(-q_\alpha^0)\hat{p}/\hbar}|n\rangle = e^{iq_\alpha^0\hat{p}/\hbar}|n\rangle$, and $n_\alpha = 0, 1, 2, \cdots, \infty$ is the quantum number for the PFS. Further, $\hat{b}_\alpha^\dagger = (\sqrt{\frac{\omega_c}{\hbar}}\hat{q}_\alpha' + i\sqrt{\frac{1}{\hbar\omega_c}}\hat{p})/\sqrt{2}$ and $\hat{b}_\alpha = (\sqrt{\frac{\omega_c}{\hbar}}\hat{q}_\alpha' - i\sqrt{\frac{1}{\hbar\omega_c}}\hat{p})/\sqrt{2}$ are the creation and annihilation operators of the PFS $|n_\alpha\rangle$, with the photon field momentum operator $\hat{p}$ and polarized photon field coordinate operator $\hat{q}_\alpha' = \hat{q} + q_\alpha^0(\mathbf{R})$. Compared to the vacuum's Fock state $|n\rangle$, these PFSs depend on the diabatic state (or more generally, the eigenstate of $\hat{\boldsymbol{\mu}}$ in a truncated electronic subspace) of the molecule, and the position of the nuclei (through the $\mathbf{R}$ dependence in $\boldsymbol{\mu}_\alpha(\mathbf{R})$). Because of the electronic state-dependent nature of the polarization (from the difference between $\boldsymbol{\mu}_I$ and $\boldsymbol{\mu}_C$), the PFS associated with different electronic diabatic states becomes nonorthogonal, i.e., $\langle n_I|m_C\rangle \neq \delta_{nm}$. Under the special case of the atomic cavity QED, the PFS representation reduces to the qubit-shifted Fock basis $\{|n_+\rangle, |m_-\rangle\}$, which has been used to solve the polariton eigen-spectrum for the quantum Rabi model[24−26,55] throughout the entire range of light−matter coupling and derive the generalized rotating-wave approximation.[24,25,54] These nonorthogonal Fock states and their overlap $\langle m_-|n_+\rangle$ have shown to effectively capture the light−matter interactions in a quantum Rabi model.[24,25]

Although the PFS appears to be related to the polarized vacuum states,[23] they are fundamentally different, with the latter one having all Fock states orthogonal to each other. Another key difference is that $|n_\alpha(\mathbf{R})\rangle$ does not parametrically depend on the positions of electrons $\hat{r}$ (hence $\langle m_I|\nabla_r|n_I\rangle = 0$), while it does depend on the diabatic state $|\alpha\rangle$, and parametrically depends on the nuclear position R such that $\langle m_I|\nabla_R|n_I\rangle \neq 0$. The polarized vacuum states, on the other hand, do parametrically depend on both electronic position $\mathbf{r}$ and the nuclear position R (see the Supporting Information for more details). For a given molecular system, one may have to consider more than two electronic states to obtain an accurate description of the polaritonic dynamics.[56,57] The PFS can be easily generalized for an arbitrary number of electronic states (see details in the Supporting Information). When approaching to a complete electronic state limit, while the eigenfunction of the dipole operator becomes the eigenfunction of (electronic and nuclear) coordinator operators, PFS remains to be fundamentally different than the polarized vacuum states defined in ref 23 (see more detailed discussion in the Supporting Information).

With the basis $|\alpha, n_\alpha\rangle \equiv |\alpha\rangle \otimes |n_\alpha(\mathbf{R})\rangle$, we evaluate the matrix elements of the PF Hamiltonian $\hat{H} = \hat{T}_\mathbf{R} + \hat{H}_{pl}$. In the Supporting Information, we offer an alternative way of obtaining these elements by using the vacuum's Fock state and applying a polaron-type transformation,[12] $\hat{U}_{pol}^\dagger\hat{H}\hat{U}_{pol}$, where $\hat{U}_{pol} = \exp\left[\frac{i}{\hbar}\sum_\alpha q_\alpha^0(\mathbf{R})|\alpha\rangle\langle\alpha|\hat{p}\right]$ is the above-mentioned photonic coordinate displacement operator. When approaching to infinite Fock states limit when $m_C \to \infty$ and $n_I \to \infty$, the basis becomes overcomplete, because $|n_I\rangle$ can be represented by $\{|m_C\rangle\}$. For a practical calculation, on the other hand, one often needs only a few of these PFSs, regardless of the coupling strength.[24−26,55]

Under the $|\alpha, n_\alpha\rangle$ representation, $\hat{H}_{pl}$ is expressed as

$$\hat{H}_{pl} = \sum_{\alpha,n_\alpha}\left(V_\alpha(\mathbf{R}) + \left(n_\alpha + \frac{1}{2}\right)\hbar\omega_c\right)|\alpha, n_\alpha\rangle\langle n_\alpha, \alpha| + \sum_{n_I,m_C}\langle m_C|n_I\rangle V_{IC}(\mathbf{R})(|I, n_I\rangle\langle m_C, C| + |C, m_C\rangle\langle n_I, I|) \tag{12}$$

Note that there is a finite coupling between the ionic state with n photons and the covalent state with m photons through the $\langle m_C|n_I\rangle V_{IC}(\mathbf{R})$ term, which is the diabatic electronic coupling $V_{IC}(\mathbf{R})$ scaled by the overlap $\langle m_C|n_I\rangle$ of the PFS. Thus, instead of having an explicit light−matter interaction term $\boldsymbol{\chi}\cdot\hat{\boldsymbol{\mu}}(\hat{a}^\dagger + \hat{a})$ (and the DSE) as shown in eq 1, these interactions are now carried through $\langle m_C|n_I\rangle V_{IC}(\mathbf{R})$.

Further, $\hat{T}_\mathbf{R}$ in the $|\alpha, n_\alpha\rangle$ basis is given by

$$\hat{T}_\mathbf{R} = \frac{1}{2\mathbf{M}}\left(\hat{P} - i\hbar\sum_{\alpha,n_\alpha,m_\alpha}\mathbf{d}_{m_\alpha n_\alpha}|\alpha, m_\alpha\rangle\langle n_\alpha, \alpha|\right)^2 \tag{13}$$

where $\mathbf{d}_{m_\alpha n_\alpha} = \langle m_\alpha|\nabla_\mathbf{R}|n_\alpha\rangle$ originated from the R-dependence of PFS, similar to the expression of the matter Hamiltonian in its electronic adiabatic representation expressed in eq 4. Note that there is no nonadiabatic couplings between states with different diabatic characters, because $\langle C, n_C|\nabla_\mathbf{R}|I, m_I\rangle = \langle n_C|\nabla_\mathbf{R}|m_I\rangle\langle C|I\rangle = 0$ (because we assume that $|I\rangle$ and $|C\rangle$ are strict diabatic basis), and they are orthogonal $\langle C|I\rangle = 0$. The polaritonic nonadiabatic coupling can be analytically evaluated (see details in the Supporting Information) as follows

$$\langle m_\alpha|\nabla_\mathbf{R}|n_\alpha\rangle = -\frac{\boldsymbol{\chi}}{\hbar\omega_c}\cdot\nabla_\mathbf{R}\boldsymbol{\mu}_\alpha(\mathbf{R})\langle m_\alpha|\hat{b}^\dagger - \hat{b}|n_\alpha\rangle \tag{14}$$

Thus, these terms couple off-resonant states that are separated by $\hbar\omega_c$ through the $(\hat{b}^\dagger - \hat{b})$ term. Further, this nonadiabatic coupling plays a similar role as the vector potential does in the Coulomb gauge. Upon a unitary transformation (see details in the Supporting Information) $\hat{U}_\theta = \exp\left[-i\frac{\pi}{2}\sum_\alpha \hat{b}_\alpha^\dagger\hat{b}_\alpha|\alpha\rangle\langle\alpha|\right]$, $\hat{H}' = \hat{U}_\theta^\dagger\hat{H}_{pl}\hat{U}_\theta$ adapts the "p·A" form of the QED Hamiltonian, where *only* the nuclear momentum operator is shifted with the amount of polarized vector potential

https://dx.doi.org/10.1021/acs.jpclett.0c02399
J. Phys. Chem. Lett. 2020, 11, 9215−9223

$\mathbf{A}_\alpha = \chi(\hat{b}_\alpha^\dagger + \hat{b}_\alpha)/\omega_c$ coupled to $\nabla_{\mathbf{R}}\boldsymbol{\mu}_\alpha(\mathbf{R})$. This form has recently shown to be the Coulomb gauge QED Hamiltonian under the electronic state truncation.[47]

We conjecture that the basis $\{|\mathrm{I}, n_\mathrm{I}\rangle, |\mathrm{C}, m_\mathrm{C}\rangle\}$ is both more computationally economic and conceptually intuitive than the conventional adiabatic-Fock states $|g, n\rangle, |e, m\rangle$. We emphasize that if we choose the same number of Fock states $\mathcal{K}$ for each electronic states, then either using vacuum's Fock states or PFS results in the same size of the Hilbert subspace for the electronic-photonic subsystem. More specifically, the electronic-photonic basis is $\{|g, 0\rangle, ..., |g, \mathcal{K}\rangle, |e, 0\rangle, ..., |e, \mathcal{K}\rangle\}$ for the adiabatic-Fock representation, and $\{|\mathrm{I}, 0_\mathrm{I}\rangle, ..., |\mathrm{I}, \mathcal{K}_\mathrm{I}\rangle, |\mathrm{C}, 0_\mathrm{C}\rangle, ..., |\mathrm{C}, \mathcal{K}_\mathrm{C}\rangle\}$ for the MH-PFS representation, both of which have exactly the same dimensions, except that the PFS has a shifted center according to the permanent dipole of the corresponding MH diabatic state. This argument can be generalized to an arbitrary number of electronic states. For numerical efficiency, we find that one needs only a few of $|\alpha, n_\alpha\rangle$ basis to converge the results of solving eq 1, whereas one needs 2−20 times more vacuum's Fock states in the range of parameters used here. This is because the vacuum's Fock states centers around $q = 0$, whereas the PFS centered around $-q_\alpha^0$. One will need a lot of $|n\rangle$ to represent the hybrid system that involves light−matter interaction with a potential centered around $-q_\alpha^0$ (see eq 11), but much fewer PFSs.

In addition, the PFS is an entangled basis between photon and matter, because it depends on both electronic state $|\alpha\rangle$ and nuclear position $\mathbf{R}$, and hence, it is well-suited for describing strong couplings among them. Previous work of using extended coherent states[58] or tunable coherent states[22] has also shown an advantage over the vacuum's Fock representation because they automatically include many-body correlations among infinitely many photons in the cavity mode.[22] However, these representations do not include matter-photon entanglement. More detailed numerical studies are necessary in the future to fully compare and assess their numerical efficiencies.

Conceptually, PFS allows one to intuitively understand the existence of certain light induced avoided crossing which is not predicted by the Rabi model. To demonstrate these effects, we use a well parametrized diabatic model of the LiF molecule[53] to investigate the molecule-cavity QED enabled new phenomena. All of the parameters for this model are directly adapted from ref 53.

Figure 1a presents the diabatic potentials energy surface $V_\alpha(R)$ of the $|\mathrm{I}\rangle$ state (red) and $|\mathrm{C}\rangle$ state (blue) in a LiF molecule, respectively. The crossing of these two *diabatic* curves occur at $R = R_0 \approx 13.5$ au, forming an avoided crossing between the adiabatic states $|g\rangle$ and $|e\rangle$ (not shown here). The diabatic coupling is $V_{\mathrm{IC}}(R)$ (gold line).

Figure 1b presents the matrix elements of $\hat{\boldsymbol{\mu}}$ in both the diabatic (solid lines) and the adiabatic (dashed lines) representations. The ionic permanent dipole (solid red) $\boldsymbol{\mu}_\mathrm{I}(R)$ increases linearly with R, while the covalent permanent dipole (solid blue) $\boldsymbol{\mu}_\mathrm{C}(R) \approx 0$, as one expects. The adiabatic states switch their characters around R_0, and as a result, the adiabatic permanent dipole switches in that region and $\mu_{eg}(R)$ peaks at R_0 as the two diabatic states couple strongly around R_0.

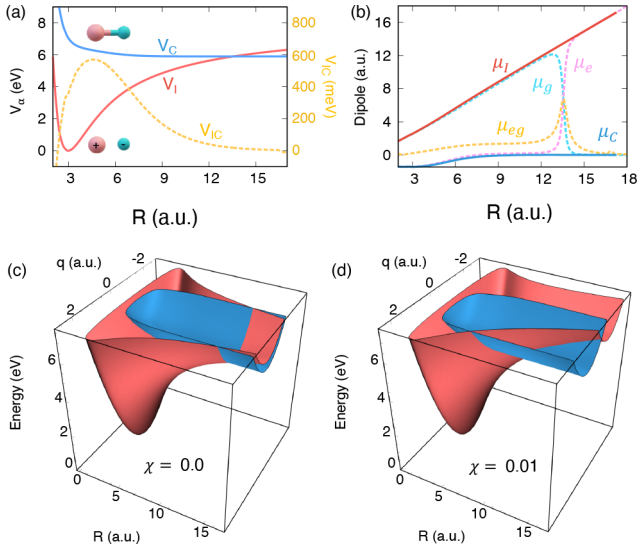

Figure 1. LiF model molecular system. (a) Diabatic potentials $V_\mathrm{I}(R)$ (red) and $V_\mathrm{C}(R)$ (blue), with diabatic coupling V_{IC} (gold line). (b) Matrix elements of $\hat{\mu}$ in the adiabatic representation (dashed curves) μ_{gg} (pink), μ_{ee} (cyan), and μ_{eg} (gold), as well as in the diabatic representation (solid lines) μ_I (red) and μ_C (blue). Cavity diabatic potentials $V_\alpha(R) + \frac{\omega_c^2}{2}(\hat{q} + q_\alpha^0(R))^2$ for the $|\alpha\rangle = |\mathrm{I}\rangle$ (blue) and $|\alpha\rangle = |\mathrm{C}\rangle$ (red) as a function of the nuclear coordinate R and the photonic coordinate q at (c) $\chi = 0.0$ and (d) $\chi = 0.007$ au.

Figure 1c demonstrates the electronic state-dependent photon field polarization by visualizing the cavity diabatic surface $\langle\alpha|(\hat{H}_{\mathrm{PF}} - \hat{T}_R - \frac{\hat{p}^2}{2})|\alpha\rangle = V_\alpha(R) + \frac{\omega_c^2}{2}(\hat{q} + q_\alpha^0(R))^2$. These diabatic surfaces are defined similarly as the cavity BO surface,[9,59] with the difference that here we project the $\left(\hat{H}_{\mathrm{PF}} - \hat{T}_R - \frac{\hat{p}^2}{2}\right)$ operator onto the MH diabatic surfaces as opposed to the electronic adiabatic surfaces. These cavity diabatic surfaces are depicted as a function of R and q, at $\chi = 0.0$ au and 0.01 au with $\hbar\omega_c = 7.5$ eV. The surfaces are color-coded corresponding to their *diabatic* electronic characters $|\mathrm{I}\rangle$ (blue) and $|\mathrm{C}\rangle$ (red). In the no coupling scenario at $\chi = 0.0$, the photon field corresponds to the vacuum photon field regardless of the electronic state. Therefore, the surfaces along the photon coordinate is a harmonic potential centered at 0. Meanwhile, at $\chi = 0.01$ au in Figure 1d the covalent diabatic surface along q is not displaced because $\mu_\mathrm{C}(R)$ is nearly zero, and the ionic cavity diabatic surface is increasingly displaced along q with an increasing R, because $\mu_\mathrm{I}(R)$ increases linearly along R. At a larger R, the extent of the photon field polarization is significantly different for the $|\mathrm{I}\rangle$ and $|\mathrm{C}\rangle$ states.

Figure 2 demonstrates that the PFS can be used to intuitively understand how a single molecular excitation can be converted into multiple excitations in the cavity, *i.e*, a down-conversion process through light−matter interactions. It can be seen from eq 12 that the covalent state with zero photons $|\mathrm{C}, 0_\mathrm{C}\rangle$ couples to $|\mathrm{I}, n_\mathrm{I}\rangle$ through the coupling $V_{\mathrm{IC}}(R)\langle 0_\mathrm{C}|n_\mathrm{I}\rangle$. Figure 2a presents the polaritonic potential energy surfaces with $\chi = 0.007$ au and $\hbar\omega_c = 1.5$ eV. The polariton potential $E_j(R)$ associated with the state $|\Phi_j(R)\rangle$ (see eq 5) is color-coded according to the expectation value of the number of photons $\langle\hat{N}\rangle = \langle\Phi_j(R)|\sum_\alpha \hat{b}_\alpha^\dagger\hat{b}_\alpha|\alpha\rangle\langle\alpha|\Phi_j(R)\rangle$, where $\hat{b}_\alpha^\dagger$ and $\hat{b}_\alpha$ are the creation and annihilation operator of the PFS (see eq

https://dx.doi.org/10.1021/acs.jpclett.0c02399
J. Phys. Chem. Lett. 2020, 11, 9215−9223

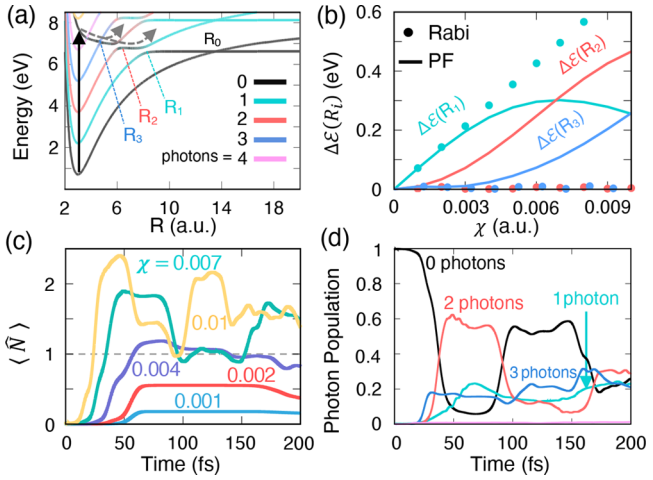

Figure 2. Using state-dependent polarization to perform down-conversion. (a) Polaritonic potentials color-coded according to the number of photons with four relevant avoided crossings labeled as R_0–R_3. The black solid vertical arrow indicates the initial photoexcitation, and the dashed lines illustrate the dynamics of the hybrid system. (b) The energy-splitting at three avoided crossings as a function of χ computed from Pauli–Fierz and Rabi Hamiltonian. (c) Time-dependent expectation value of the number of photons at various χ. (d) Time-dependent photon populations at χ = 0.007 au.

11), where $\alpha \in \{\mathrm{I}, \mathrm{C}\}$. We emphasize that for the PF QED Hamiltonian under the dipole gauge, $\langle \hat{N} \rangle = \langle \sum_\alpha \hat{b}_\alpha^\dagger \hat{b}_\alpha |\alpha\rangle\langle\alpha| \rangle$ is the physically meaningful way to characterize the number of photons.[60] This is because $\hat{N}_c = \hat{a}^\dagger \hat{a}$ is the correct photon number operator under the *Coulomb* gauge. When calculating this quantity under the dipole gauge for the PF Hamiltonian, the operator should also be gauge transformed[46,60] (for the case of the PF Hamiltonian, both the PZW and a phase transformation), resulting in $\hat{N} = \sum_\alpha \hat{b}_\alpha^\dagger \hat{b}_\alpha |\alpha\rangle\langle\alpha|$. Under the dipole gauge, using $\langle \hat{N}_c \rangle = \langle \hat{a}^\dagger \hat{a} \rangle$ gives an unphysical measure of the photon number.[46,60]

In Figure 2a, several new light-induced avoided crossings (LIAC) at R_1, R_2, and R_3 are formed because of the light–matter interactions, in addition to the original electronic avoided crossing at R_0.

Figure 2b presents the energy-splitting $\Delta\mathcal{E}(R_i)$ associated with three cavity-induced avoided crossings at R_1, R_2, and R_3 as a function of χ. Here, we compare these energy splittings computed from both the Rabi (filled circles) and the Pauli–Fierz Hamiltonian (solid lines). For the Rabi model in the adiabatic-Fock representation ($\{|g, n\rangle, |e, n\rangle\}$), one ignores the permanent dipole contribution ($\boldsymbol{\mu}_{ee}$ and $\boldsymbol{\mu}_{gg}$), as well as all of the DSE terms. The Rabi model is widely used in recent molecular polariton chemistry investigations.[5,13,14,16,22] While the Rabi model provides a reasonable description of $\Delta\mathcal{E}(R_1)$ at weak coupling, it fails to correctly describe $\Delta\mathcal{E}(R_1)$ at a larger coupling strength and failed to predict $\Delta\mathcal{E}(R_2)$ and $\Delta\mathcal{E}(R_3)$. This is because these deviations are caused by permanent dipole moments $\boldsymbol{\mu}_{gg}$ and $\boldsymbol{\mu}_{ee}$. For example, to explain $\Delta\mathcal{E}(R_2)$ in the adiabatic-Fock basis $\{|g, n\rangle, |e, m\rangle\}$, it is straightforward to recognize that $|g, 2\rangle$ couples with $|g, 1\rangle$ through $\langle g, 2|\hat{\boldsymbol{\mu}}(\hat{a}^\dagger + \hat{a})|g, 1\rangle = \boldsymbol{\mu}_{gg}\langle 2|(\hat{a}^\dagger + \hat{a})|1\rangle$, and $|g, 1\rangle$ couples to the $|e, 0\rangle$ through $\boldsymbol{\mu}_{ge}\langle 1|(\hat{a}^\dagger + \hat{a})|0\rangle$. Hence, the Rabi model that ignores the permanent dipole will not give a correct prediction. Under the usual Fock state basis, it is not conceptually intuitive to discuss the role of $\boldsymbol{\mu}_{gg}$ and $\boldsymbol{\mu}_{ee}$. Under the PFS basis, on the other hand, it is intuitive to understand these phenomena, and this coupling can be simply estimated as $V_{\mathrm{IC}}\langle n_{\mathrm{C}}|m_{\mathrm{I}}\rangle$, which means $\Delta\mathcal{E}(R_2) = 2V_{\mathrm{IC}}\langle 2_{\mathrm{I}}|0_{\mathrm{c}}\rangle$ at the resonance nuclear configuration R_2 where $V_{\mathrm{I}}(R_2) + 2\hbar\omega_{\mathrm{c}} = V_{\mathrm{C}}(R_2)$ (when ignoring other nonresonance couplings). In the Supporting Information, we further demonstrate that these simple analytic expressions of $\langle n_{\mathrm{C}}|m_{\mathrm{I}}\rangle$ provide almost an exact answer for $\Delta\mathcal{E}(R_i)$ presented in this panel. As an example, $\Delta\mathcal{E}(R_1) = 2\langle 0_{\mathrm{c}}|1_{\mathrm{I}}\rangle = 2\left(\frac{\chi\cdot\Delta\boldsymbol{\mu}}{\hbar\omega_{\mathrm{c}}}\right)\exp\left[-\frac{1}{2}\frac{(\chi\cdot\Delta\boldsymbol{\mu})^2}{(\hbar\omega_{\mathrm{c}})^2}\right]$ with $\Delta\boldsymbol{\mu} = \boldsymbol{\mu}_{\mathrm{I}} - \boldsymbol{\mu}_{\mathrm{C}}$. This expression captures both the linear increase of $\Delta\mathcal{E}$ at a weak χ (as predicted by the Rabi model) as well as the exponential decay of it at a larger χ. Note that in the atomic quantum optics literature,[48] the coupling strength is characterized based on the value of $\eta = \boldsymbol{\chi}\cdot\boldsymbol{\mu}_{eg}/\omega_c$, and the ultrastrong coupling regime and deep-strong coupling regime are often defined as $0.1 < \eta < 1.0$ and $1.0 < \eta$, respectively. When $\eta > 0.1$, the JC model usually breaks down and the full Rabi model has to be considered to obtain the correct polariton eigenspectrum.[48] With this definition, considering that $\mu_{eg}(R) \approx 1.5$ au for $R \in [6, 11]$ au, the coupling χ = 0.007 au used in Figure 2a corresponds to η = 0.19. On the other hand, the Rabi model explicitly breaks down and failed to correctly predict $\Delta\mathcal{E}(R_2)$ and $\Delta\mathcal{E}(R_3)$, even when $\eta < 0.1$ ($\chi < 0.037$). Hence, the characterization of different coupling regimes needs to be carefully revisited for molecular cavity QED in the future, because the one used in atomic QED does not consider the permanent dipole or the R dependence of the transition and permanent dipoles in a molecule (as indicated in Figure 1b).

Figure 2c presents the time-dependent number of photons $\langle \hat{N} \rangle(t) = \langle \Psi(t)|\sum_\alpha \hat{b}_\alpha^\dagger \hat{b}_\alpha |\alpha\rangle\langle\alpha|\Psi(t)\rangle$ to demonstrate the down-conversion process, where $|\Psi(t)\rangle$ is the total wave function of the hybrid molecule–cavity system. The initial condition is $|\Psi(0)\rangle \sim \exp(-\alpha(R - R_g)^2) \otimes |\Phi_5(R)\rangle$, where $|\Phi_5(R)\rangle \approx |\mathrm{C}, 0_{\mathrm{C}}\rangle$ in the Franck–Condon region. The initial wavepacket is centered at R_g = 3.01 au and a width α = 19.12 au to mimic a vertical Franck–Condon excitation of the molecule-cavity hybrid system from its ground state. In the range of parameters used here, $\langle \hat{N} \rangle(t)$ reaches as high as 2.4, representing multiple photons created per molecular excitation. The maximum value for $\langle \hat{N} \rangle(t)$ also increases with a higher χ.

Figure 2d presents the population of the polarized Fock states $P_n = \langle \Psi(t)[\sum_\alpha |\alpha, n_\alpha\rangle\langle n_\alpha, \alpha|]|\Psi(t)\rangle$ at χ = 0.007 au. With this coupling strength, all of the LIAC at R_1, R_2, and R_3 become considerably large. Hence, the wavepacket first branches at R_3, then at R_2 and finally at R_1, leading to sequential rising of the 3-photon (blue), 2-photon (red), and 1-photon populations (green). This demonstrates the possibility of converting molecular excitation to multiple photons. It is also possible to selectively control the number of photons by changing χ. More detailed discussion of the population dynamics is provided in the Supporting Information, together with the results in the polariton basis $|\Phi_j(R)\rangle$. Note that the down-conversion presented here is enabled because of the coupling between the $|\mathrm{I}, n_{\mathrm{I}}\rangle$ (for $n \geq 2$) and $|\mathrm{C}, 0_{\mathrm{C}}\rangle$ states (and between $|g, n\rangle$ and the $|e, 0\rangle$ state in the Fock state basis), which go beyond the prediction of the Rabi model.

https://dx.doi.org/10.1021/acs.jpclett.0c02399
J. Phys. Chem. Lett. 2020, 11, 9215–9223

These new avoided crossings are reminiscent of the avoided crossings in opto-mechanical systems when quantizing the mirror motion to describe the dynamical Casimir effect.[61,62] For example, in the opto-mechanical system, it was found that avoided crossings are created by hybridizing the $|1_{mir}, 0\rangle$ state (mirror motion is excited, and 0 photons in the cavity) and $|0_{mir}, 2\rangle$ state (mirror motion is in the ground state, and 2 photons in the cavity). These two states are coupled, leading to two-photon emission out of vacuum by converting a single excitation of the mirror.[61] This behavior is similar to the avoided crossing created between $|I, 2_I\rangle$ and $|C, 0_C\rangle$ in the current study of molecular cavity QED.

Further, we do not expect the cavity loss to impede this down-conversion process. This is because, before the spontaneous emission happened (which is induced by the quantum transition from the $|C, 0_C\rangle$ state to the $|I, n_I\rangle$ state), the nuclear wavepacket is traveling in the polaritonic state that has a molecular excitation character, which is robust to the cavity loss. The transition between the $|C, 0_C\rangle$ state to the $|I, n_I\rangle$ state happens within 5−10 fs (as indicated in Figure 2d), and once it occurs, the molecule emits n photons inside the cavity. Whether these photons are confined inside the cavity or leaked outside the cavity does not change the fact that multiple photons were generated. On the other hand, the cavity loss could impact the reabsorption process of the molecule at ∼100 fs in Figure 2d, indicated by the black solid line going up and the red solid line coming down.

The polarized Fock states associated with different electronic states are nonorthogonal to each other. This nonorthogonality leads to the generation of multiple photons, similar to the dynamical Casimir effect[63−67] where the fast displacement of the cavity mirrors breaks the orthogonality of the Fock states because of the changing of boundary conditions, converting virtual photons into real photons. Experimentally, the dynamical Casimir effect has been demonstrated by effectively altering the boundary conditions through certain system parameters (such as the refractive index[68,69]) instead of physically moving mirrors which was suggested to require a very fast speed of mirror vibrations (approaching the relativistic limit).[67,69,70] Recently, it was suggested that by coupling a three-level atom[71] or a photoisomerization molecule[13] to the cavity, one can achieve similar effects of DCE by generating more than one photon from a single excitation. The scenario we present here, however, relies on only a simple two-state diatomic molecule couple to the cavity and operates on a similar mechanics of breaking the orthogonality among Fock states, through molecular vibrations instead of the mechanical motion of the mirror.

Figure 3 demonstrates that the electronic nonadiabatic coupling at R_0 is modified through the light−matter interactions, which can be intuitively understood through the nonorthogonality of the PFS theoretical framework, leading to the enhancement of the photodissociation dynamics. To clearly show this, we choose a high photon frequency $\hbar\omega_c$ = 7.5 eV, such that all of the other polariton states are above $|\Phi_1(R)\rangle$ throughout the dynamically relevant parts of R. Figure 3a presents the first three polaritonic potentials $E_j(R)$ of the hybrid system with the inset depicting the polariton potentials $E_0(R)$ and $E_1(R)$ at different χ. The polaritonic potentials of the $|\Phi_0(R)\rangle$ and $|\Phi_1(R)\rangle$ states are nearly identical to the original molecular adiabatic potentials of $|g\rangle$ and $|e\rangle$ state. At χ = 0, the energy-splitting between $|\Phi_0(R)\rangle$ and $|\Phi_1(R)\rangle$

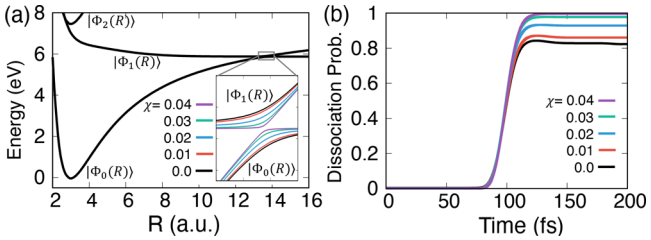

Figure 3. Controlling photochemical reactions with photon field polarization. (a) Polaritonic potentials with a high photon frequency $\hbar\omega_c$ = 7.5 eV, with the inset showing the lowest two polaritonic potentials near R_0 at various χ. (b) Dissociation probability at various χ.

corresponds to the bare molecular system, given by $2V_{IC}(R_0)$. By increasing χ we see a clear trend of decreasing the energy-splitting, as indicated in the inset. The splitting between the two states is given by $V_{IC}(R)\langle 0_c|0_I\rangle = V_{IC}(R)\exp\{-1/2[\chi\Delta\mu_{IC}(R_0)/\hbar\omega_c]^2\}$ (ignoring all other off-resonant contributions), where $\Delta\mu_{IC}(R_0) = \mu_I(R_0) - \mu_C(R_0)$. Thus, increasing χ effectively decreases $\Delta\mathcal{E}(R_0)$, causing the nonadiabatic coupling $\langle\Phi_0(R)|\nabla_R|\Phi_1(R)\rangle$ to increase (see the Supporting Information).

Figure 3b presents the photodissociation dynamics of the LiF molecule defined as $\langle\Psi(t)|\Phi_0(R)\rangle\langle\Phi_0(R)|\Theta(R - R_0)|\Psi(t)\rangle$, where Θ is the Heaviside function. The initial quantum state is $|\Psi(t = 0)\rangle \sim \exp(-\alpha(R - R_g)^2) \otimes |\Phi_1(R)\rangle$. The dissociation occurs by making a nonadiabatic transition from the initially occupied $|\Phi_1(R)\rangle$ state to the dissociative $|\Phi_0(R)\rangle$ state around the R_0 region. An increase in χ leads to a decrease in energy splitting and an increase in the nonadiabaticity, which results in a larger nonadiabatic transition probability. Therefore, enhanced dissociation dynamics occurs from increasing the light−matter coupling χ. This is a fundamentally different scenario compared to the situation in Figure 2, where increasing the light−matter coupling strength leads to suppression of the dissociation of the molecule by preventing it approaching to the electronic avoided crossing at R_0.

Despite several existing works on controlling chemical reactivity through molecule−cavity coupling[5,10,11,16,72,73] that relied on introducing new nonadiabatic couplings through resonance light−matter interactions, the control scheme demonstrated here is fundamentally different. Here, we modify the original electronic nonadiabatic coupling through off-resonance light−matter interactions. Because of the choice of an off-resonant photon mode, no cavity photons are emitted to modify the chemical reactivity, in contrast to most of the previous works.[5,10,11,16,72,73] Thus, the cavity loss is expected to play a minimal role in the polariton photochemistry dynamics presented here.

In this work we have considered only a single-cavity radiation mode coupled to the molecular system, in order to clearly demonstrate the advantage of the PFS representation. Other radiation modes with higher frequency (overtone) inside the cavity may also play a crucial[74] role in the polaritonic dynamics, especially when considering a photon frequency that is much lower than the electronic excitation energy. We expect that the PFS representation will provide computational as well as conceptual benefits when considering many radiation modes in the optical cavity, as it provides a compact representation to quantize radiation modes. Further, we employed the long-

https://dx.doi.org/10.1021/acs.jpclett.0c02399
J. Phys. Chem. Lett. 2020, 11, 9215−9223

wavelength approximation, based on the assumption that the spatial dependence of the electromagnetic field is ignored (see the Supporting Information). This is a valid approximation for a simple Fabry−Perrot cavity for the range of photon frequencies used in this work, because the length of a LiF molecule is extremely small compared to the length of the cavity. Whether the PFS representation would provide conceptual simplicity beyond the long-wavelength approximation or if can it be extended to quantize other "photonic" quasiparticles[75] (such as plasmon polaritons or phonon polaritons) remains an open-question. Future studies will be devoted to answering them.

In conclusion, we demonstrate that the presence of the permanent dipole moments and the associated dipole self-energy terms leads to the polarization of the vacuum photon field. These polarized Fock states associated with different electronic states are nonorthogonal to each other. This nonorthogonality leads to the generation of multiple photons, which is similar to the dynamical Casimir effect[13,63−66] where the permanent dipole difference plays a similar role as the physical displacement of the cavity mirrors. Through numerically exact quantum dynamics simulations, we demonstrate the possibility to exploit this nonorthogonality to achieve multiple photon generation and to enhance the photodissociation of a molecule by coupling to a cavity. We propose that experimentally, one should be able to observe such dynamical Casimir effects by using a molecule that has large permanent dipole difference among its electronic states. Through the ultrastrong coupling between the molecule and the cavity, the molecular vibrations allow the polariton wave packet to visit nonorthogonal PFSs, leading to the conversion of multiple photons.

More importantly, we demonstrate the conceptual and computational convenience of the polarized Fock states (PFSs) in molecular cavity QED, compared to the widely used vacuum Fock states. We envision that the PFS representation will provide a powerful theoretical framework to facilitate polariton chemistry investigations.[5,10,16,44,72,73,76,77]

■ ASSOCIATED CONTENT

Supporting Information

The Supporting The Supporting Information is available free of charge at https://pubs.acs.org/doi/10.1021/acs.jpclett.0c02399.

Details of the derivation of the molecular Hamiltonian in the adiabatic representation, details of the nonadiabatic coupling between polarized Fock states and the connection to the P·A Hamiltonian, connection to the polaron transformation, details of the Mulliken−Hush diabatization for a two-level system, computational details and additional results for polariton population dynamics, generalized theory of the polarized Fock states, polarized Fock states in the infinite electronic basis limit, and the derivation of the Pauli−Fierz Hamiltonian (PDF)

■ AUTHOR INFORMATION

Corresponding Authors

Arkajit Mandal − *Department of Chemistry, University of Rochester, Rochester, New York 14627, United States;* Email: amandal4@ur.rochester.edu

Pengfei Huo − *Department of Chemistry, University of Rochester, Rochester, New York 14627, United States;* orcid.org/0000-0002-8639-9299; Email: pengfei.huo@rochester.edu

Author

Sebastian Montillo Vega − *Department of Chemistry, University of Rochester, Rochester, New York 14627, United States*

Complete contact information is available at: https://pubs.acs.org/10.1021/acs.jpclett.0c02399

Notes

The authors declare no competing financial interest.

■ ACKNOWLEDGMENTS

This work was supported by the National Science Foundation "Enabling Quantum Leap in Chemistry" program under Grant Number CHE-1836546, as well as by a Cottrell Scholar award (a program by of Research Corporation for Science Advancement). Computing resources were provided by the Center for Integrated Research Computing (CIRC) at the University of Rochester. A.M. appreciates the support from his Elon Huntington Hooker Fellowship. S.M.V. appreciates generous support from the i-scholar program of the Department of Chemistry at the University of Rochester. A.M. appreciates stimulating discussions with Wanghuai Zhou and Marwa Farag. We appreciate valuable conversations with Prof. Peter Milonni.

■ REFERENCES

(1) Hutchison, J. A.; Schwartz, T.; Genet, C.; Devaux, E.; Ebbesen, T. W. Modifying Chemical Landscapes by Coupling to Vacuum Fields. *Angew. Chem., Int. Ed.* **2012**, *51*, 1592−1596.

(2) Ebbesen, T. W. Hybrid Light-Matter States in a Molecular and Material Science Perspective. *Acc. Chem. Res.* **2016**, *49*, 2403−2412.

(3) Kowalewski, M.; Mukamel, S. Manipulating Molecules with Quantum Light. *Proc. Natl. Acad. Sci. U. S. A.* **2017**, *114*, 3278−3280.

(4) Thomas, A.; Lethuillier-Karl, L.; Nagarajan, K.; Vergauwe, R. M. A.; George, J.; Chervy, T.; Shalabney, A.; Devaux, E.; Genet, C.; Moran, J.; Ebbesen, T. W. Tilting a Ground-State Reactivity Landscape by Vibrational Strong Coupling. *Science* **2019**, *363*, 615−619.

(5) Kowalewski, M.; Bennett, K.; Mukamel, S. Cavity Femtochemistry: Manipulating Nonadiabatic Dynamics at Avoided Crossings. *J. Phys. Chem. Lett.* **2016**, *7*, 2050−2054.

(6) Kowalewski, M.; Bennett, K.; Mukamel, S. Non-adiabatic Dynamics of Molecules in Optical Cavities. *J. Chem. Phys.* **2016**, *144*, 054309.

(7) Herrera, F.; Spano, F. C. Cavity-Controlled Chemistry in Molecular Ensembles. *Phys. Rev. Lett.* **2016**, *116*, 238301.

(8) Galego, J.; Garcia-Vidal, F. J.; Feist, J. Suppressing Photochemical Reactions with Quantized Light Fields. *Nat. Commun.* **2016**, *7*, 13841.

(9) Flick, J.; Ruggenthaler, M.; Appel, H.; Rubio, A. Atoms and Molecules in Cavities, from Weak to Strong Coupling in Quantum-Electrodynamics (QED) Chemistry. *Proc. Natl. Acad. Sci. U. S. A.* **2017**, *114*, 3026−3034.

(10) Feist, J.; Galego, J.; Garcia-Vidal, F. J. Polaritonic Chemistry with Organic Molecules. *ACS Photonics* **2018**, *5*, 205−216.

(11) Csehi, A.; Kowalewski, M.; Halász, G. J.; Vibók, Á. Ultrafast Dynamics in the Vicinity of Quantum Light-Induced Conical Intersections. *New J. Phys.* **2019**, *21*, 093040.

(12) Semenov, A.; Nitzan, A. Electron Transfer in Confined Electromagnetic Fields. *J. Chem. Phys.* **2019**, *150*, 174122.

(13) Pérez-Sánchez, J. B.; Yuen-Zhou, J. Polariton Assisted Down-Conversion of Photons via Nonadiabatic Molecular Dynamics: A Molecular Dynamical Casimir Effect. *J. Phys. Chem. Lett.* **2020**, *11*, 152−159.
(14) Mandal, A.; Huo, P. Investigating New Reactivities Enabled by Polariton Photochemistry. *J. Phys. Chem. Lett.* **2019**, *10*, 5519−5529.
(15) Galego, J.; Climent, C.; Garcia-Vidal, F. J.; Feist, J. Cavity Casimir-Polder Forces and Their Effects in Ground-State Chemical Reactivity. *Phys. Rev. X* **2019**, *9*, 021057.
(16) Vendrell, O. Coherent Dynamics in Cavity Femtochemistry: Application of the Multi-Configuration Time-Dependent Hartree Method. *Chem. Phys.* **2018**, *509*, 55−65.
(17) Gu, B.; Mukamel, S. Manipulating Nonadiabatic Conical Intersection Dynamics by Optical Cavities. *Chem. Sci.* **2020**, *11*, 1290−1298.
(18) Du, M.; Ribeiro, R. F.; Yuen-Zhou, J. Remote Control of Chemistry in Optical Cavities. *Chem.* **2019**, *5*, 1167−1181.
(19) Szidarovszky, T.; Halász, G. J.; Császár, A. G.; Cederbaum, L. S.; Vibók, A. Conical Intersections Induced by Quantum Light: Field-Dressed Spectra from the Weak to the Ultrastrong Coupling Regimes. *J. Phys. Chem. Lett.* **2018**, *9*, 6215−6223.
(20) Jaynes, E.; Cummings, F. Comparison of Quantum and Semiclassical Radiation Theories With Application to the Beam Maser. *Proc. IEEE* **1963**, *51*, 89−109.
(21) Tavis, M.; Cummings, F. Exact Solution for an N-Molecule-Radiation-Field Hamiltonian. *Phys. Rev.* **1968**, *170*, 379−384.
(22) Bennett, K.; Kowalewski, M.; Mukamel, S. Novel Photochemistry of Molecular Polaritons in Optical Cavities. *Faraday Discuss.* **2016**, *194*, 259−282.
(23) Schäfer, C.; Ruggenthaler, M.; Rubio, A. Ab Initio Nonrelativistic Quantum Electrodynamics: Bridging Quantum Chemistry and Quantum Optics From Weak to Strong Coupling. *Phys. Rev. A: At., Mol., Opt. Phys.* **2018**, *98*, 043801.
(24) Irish, E. K.; Gea-Banacloche, J.; Martin, I.; Schwab, K. C. Dynamics of a Two-Level System Strongly Coupled to a High-Frequency Quantum Oscillator. *Phys. Rev. B: Condens. Matter Mater. Phys.* **2005**, *72*, 195410.
(25) Irish, E. K. Generalized Rotating-Wave Approximation for Arbitrarily Large Coupling. *Phys. Rev. Lett.* **2007**, *99*, 173601.
(26) Albert, V. V.; Scholes, G. D.; Brumer, P. Symmetric Rotating-Wave Approximation for the Generalized Single-Mode Spin-Boson System. *Phys. Rev. A: At., Mol., Opt. Phys.* **2011**, *84*, 042110.
(27) Yu, L.; Zhu, S.; Liang, Q.; Chen, G.; Jia, S. Analytical Solutions for the Rabi Model. *Phys. Rev. A: At., Mol., Opt. Phys.* **2012**, *86*, 015803.
(28) Meath, W. J.; Power, E. A. On the Importance of Permanent Moments in Multiphoton Absorption Using Perturbation Theory. *J. Phys. B: At. Mol. Phys.* **1984**, *17*, 763−781.
(29) Thomas, G. F. Effects of Permanent Dipole Moments on the Collision-Free Interaction of a Two-Level System With a Laser and a Static Electric Field. *Phys. Rev. A: At., Mol., Opt. Phys.* **1986**, *33*, 1033−1038.
(30) Kibis, O. V.; Slepyan, G. Y.; Maksimenko, S. A.; Hoffmann, A. Matter Coupling to Strong Electromagnetic Fields in Two-Level Quantum Systems with Broken Inversion Symmetry. *Phys. Rev. Lett.* **2009**, *102*, 023601.
(31) Meath, W. J.; Power, E. A. On the Effects of Diagonal Dipole Matrix Elements in Multi-Photon Resonance Profiles Using Two-Level Systems As Models. *Mol. Phys.* **1984**, *51*, 585−600.
(32) Bavli, R.; Heller, D. F.; Band, Y. B. Nonlinear-Optical Properties of Two-Level Systems With Permanent Dipole Moments. *Phys. Rev. A: At., Mol., Opt. Phys.* **1990**, *41*, 3960−3968.
(33) Macovei, M.; Mishra, M.; Keitel, C. H. Population Inversion in Two-Level Systems Possessing Permanent Dipoles. *Phys. Rev. A: At., Mol., Opt. Phys.* **2015**, *92*, 013846.
(34) Baranov, D. G.; Petrov, M. I.; Krasnok, A. E. Decoupling Light and Matter: Permanent Dipole Moment Induced Collapse of Rabi Oscillations. *arXiv* **2016**, 1611.06897.
(35) Lacombe, L.; Hoffmann, N. M.; Maitra, N. T. Exact Potential Energy Surface for Molecules in Cavities. *Phys. Rev. Lett.* **2019**, *123*, 083201.
(36) Szidarovszky, T.; Halász, G. J.; Vibok, A. Three-Player Polaritons: Nonadiabatic Fingerprints in an Entangled Atom−Molecule−Photon System. *New J. Phys.* **2020**, *22*, 053001.
(37) Rokaj, V.; Welakuh, D. M.; Ruggenthaler, M.; Rubio, A. Light−Matter Interaction in the Longwavelength Limit: No Ground-State Without Dipole Self-Energy. *J. Phys. B: At., Mol. Opt. Phys.* **2018**, *51*, 034005.
(38) Mandal, A.; Krauss, T. D.; Huo, P. Polariton-Mediated Electron Transfer via Cavity Quantum Electrodynamics. *J. Phys. Chem. B* **2020**, *124*, 6321−6340.
(39) Power, E. A.; Zienau, S. Coulomb Gauge in Non-relativistic Quantum Electro-Dynamics and the Shape of Spectral Lines. *Philos. Trans. R. Soc. London, Ser. A* **1959**, *251*, 427−454.
(40) Cohen-Tannoudji, C.; Dupont-Roc, J.; Grynberg, G. *Photons and Atoms: Introduction to Quantum Electrodynamics*. John Wiley & Sons, Inc.: Hoboken, NJ, 1989.
(41) Pacher, T.; Mead, C. A.; Cederbaum, L. S.; Koppel, H. Gauge Theory and Quasidiabatic States in Molecular Physics. *J. Chem. Phys.* **1989**, *91*, 7057.
(42) Worth, G. A.; Cederbaum, L. S. Beyond Born-Oppenheimer: Molecular Dynamics Through a Conical Intersection. *Annu. Rev. Phys. Chem.* **2004**, *55*, 127−158.
(43) Galego, J.; Garcia-Vidal, F. J.; Feist, J. Cavity-Induced Modifications of Molecular Structure in the Strong-Coupling Regime. *Phys. Rev. X* **2015**, *5*, 041022.
(44) Zhang, Y.; Nelson, T.; Tretiak, S. Non-Adiabatic Molecular Dynamics of Molecules in the Presence of Strong Light-Matter Interactions. *J. Chem. Phys.* **2019**, *151*, 154109.
(45) De Bernardis, D.; Pilar, P.; Jaako, T.; De Liberato, S.; Rabl, P. Breakdown of Gauge Invariance in Ultrastrong-Coupling Cavity QED. *Phys. Rev. A: At., Mol., Opt. Phys.* **2018**, *98*, 053819.
(46) Di Stefano, O.; Settineri, A.; Macri, V.; Garziano, L.; Stassi, R.; Savasta, S.; Nori, F. Resolution of Gauge Ambiguities in Ultrastrong-Coupling Cavity Quantum Electrodynamics. *Nat. Phys.* **2019**, *15*, 803−808.
(47) Taylor, M. A. D.; Mandal, A.; Zhou, W.; Huo, P. Resolution of Gauge Ambiguities in Molecular Cavity Quantum Electrodynamics. *Phys. Rev. Lett.* **2020**, *125*, 123602.
(48) Frisk Kockum, A.; Miranowicz, A.; De Liberato, S.; Savasta, S.; Nori, F. Ultrastrong Coupling Between Light and Matter. *Nat. Rev. Phys.* **2019**, *1*, 19−40.
(49) Mulliken, R. S. Molecular Compounds and their Spectra. II. *J. Am. Chem. Soc.* **1952**, *74*, 811−824.
(50) Cave, R. J.; Newton, M. D. Generalization of the Mulliken-Hush Treatment for the Calculation of Electron Transfer Matrix Elements. *Chem. Phys. Lett.* **1996**, *249*, 15−19.
(51) Cave, R. J.; Newton, M. D. Calculation of Electronic Coupling Matrix Elements for Ground and Excited State Electron Transfer Reactions: Comparison of the Generalized Mulliken−Hush and Block Diagonalization Methods. *J. Chem. Phys.* **1997**, *106*, 9213−9226.
(52) Hush, N. S. *Intervalence-Transfer Absorption. Part 2. Theoretical Considerations and Spectroscopic Data*. John Wiley & Sons, Inc.: Hoboken, NJ, 2007.
(53) Giese, T. J.; York, D. M. Complete Basis Set Extrapolated Potential Energy, Dipole, and Polarizability Surfaces of Alkali Halide Ion-Neutral Weakly Avoided Crossings With and Without Applied Electric Fields. *J. Chem. Phys.* **2004**, *120*, 7939−7948.
(54) Agarwal, S.; Rafsanjani, S. M. H.; Eberly, J. H. Tavis-Cummings Model Beyond the Rotating Wave Approximation: Quasidegenerate Qubits. *Phys. Rev. A: At., Mol., Opt. Phys.* **2012**, *85*, 043815.
(55) Schweber, S. On the Application of Bargmann Hilbert Spaces to Dynamical Problems. *Ann. Phys.* **1967**, *41*, 205.
(56) Flick, J.; Narang, P. Ab initio polaritonic potential-energy surfaces for excited-state nanophotonics and polaritonic chemistry. *J. Chem. Phys.* **2020**, *153*, 094116.

https://dx.doi.org/10.1021/acs.jpclett.0c02399
J. Phys. Chem. Lett. 2020, 11, 9215−9223

(57) Tóth, A.; Csehi, A.; Halász, G. J.; Vibók, A. Photodissociation dynamics of the LiF molecule: Two- and three-state descriptions. *Phys. Rev. A: At., Mol., Opt. Phys.* **2019**, *99*, 043424.
(58) Chen, Q.-H.; Wang, C.; He, S.; Liu, T.; Wang, K.-L. Exact Solvability of the Quantum Rabi Model Using Bogoliubov Operators. *Phys. Rev. A: At., Mol., Opt. Phys.* **2012**, *86*, 023822.
(59) Flick, L. J.; Appel, H.; Ruggenthaler, M.; Rubio, A. Cavity Born−Oppenheimer Approximation for Correlated Electron−Nuclear-Photon Systems. *J. Chem. Theory Comput.* **2017**, *13*, 1616−1625.
(60) Schäfer, C.; Ruggenthaler, M.; Rokaj, V.; Rubio, A. Relevance of the Quadratic Diamagnetic and Self-Polarization Terms in Cavity Quantum Electrodynamics. *ACS Photonics* **2020**, *7*, 975−990.
(61) Macrì, V.; Ridolfo, A.; Di Stefano, O.; Kockum, A. F.; Nori, F.; Savasta, S. Nonperturbative Dynamical Casimir Effect in Optomechanical Systems: Vacuum Casimir-Rabi Splittings. *Phys. Rev. X* **2018**, *8*, 011031.
(62) Settineri, A.; Macrì, V.; Garziano, L.; Di Stefano, O.; Nori, F.; Savasta, S. Conversion of Mechanical Noise Into Correlated Photon Pairs: Dynamical Casimir Effect From an Incoherent Mechanical Drive. *Phys. Rev. A: At., Mol., Opt. Phys.* **2019**, *100*, 022501.
(63) Moore, G. T. Quantum Theory of the Electromagnetic Field in a Variable-Length One-Dimensional Cavity. *J. Math. Phys.* **1970**, *11*, 2679−2691.
(64) Yablonovitch, E. Accelerating Reference Frame for Electromagnetic Waves in a Rapidly Growing Plasma: Unruh-Davies-Fulling-DeWitt Radiation and the Nonadiabatic Casimir Effect. *Phys. Rev. Lett.* **1989**, *62*, 1742−1745.
(65) Schwinger, J. Casimir Energy for Dielectrics. *Proc. Natl. Acad. Sci. U. S. A.* **1992**, *89*, 4091−4093.
(66) Dodonov, V. V. Current Status of the Dynamical Casimir Effect. *Phys. Scr.* **2010**, *82*, 038105.
(67) Wilson, C. M.; Johansson, G.; Pourkabirian, A.; Simoen, M.; Johansson, J. R.; Duty, T.; Nori, F.; Delsing, P. Observation of the Dynamical Casimir Effect in a Superconducting Circuit. *Nature* **2011**, *479*, 376−379.
(68) Dezael, F. X.; Lambrecht, A. Analogue Casimir Radiation Using an Optical Parametric Oscillator. *Europhys. Lett.* **2010**, *89*, 14001.
(69) Vezzoli, S.; Mussot, A.; Westerberg, N.; Kudlinski, A.; Dinparasti Saleh, H.; Prain, A.; Biancalana, F.; Lantz, E.; Faccio, D. Optical Analogue of the Dynamical Casimir Effect in a Dispersion-Oscillating Fibre. *Commun. Phys.* **2019**, *2*, 84.
(70) Lähteenmäki, P.; Paraoanu, G. S.; Hassel, J.; Hakonen, P. J. Dynamical Casimir Effect in a Josephson Metamaterial. *Proc. Natl. Acad. Sci. U. S. A.* **2013**, *110*, 4234−4238.
(71) Stassi, R.; Ridolfo, A.; Di Stefano, O.; Hartmann, M. J.; Savasta, S. Spontaneous Conversion from Virtual to Real Photons in the Ultrastrong-Coupling Regime. *Phys. Rev. Lett.* **2013**, *110*, 243601.
(72) Triana, J. F.; Peláez, D.; Sanz-Vicario, J. L. Entangled Photonic-Nuclear Molecular Dynamics of LiF in Quantum Optical Cavities. *J. Phys. Chem. A* **2018**, *122*, 2266−2278.
(73) Triana, J. F.; Sanz-Vicario, J. L. Revealing the Presence of Potential Crossings in Diatomics Induced by Quantum Cavity Radiation. *Phys. Rev. Lett.* **2019**, *122*, 063603.
(74) Hoffmann, N. M.; Lacombe, L.; Rubio, A.; Maitra, N. T. Effect of Many Modes on Self-Polarization and Photochemical Suppression in Cavities. *J. Chem. Phys.* **2020**, *153*, 104103.
(75) Rivera, N.; Kaminer, I. Light-Matter Interactions With Photonic Quasiparticles. *arXiv* **2020**, 2004.07748 .
(76) Rivera, N.; Flick, J.; Narang, P. Variational Theory of Nonrelativistic Quantum Electrodynamics. *Phys. Rev. Lett.* **2019**, *122*, 193603.
(77) Fregoni, J.; Granucci, G.; Coccia, E.; Persico, M.; Corni, S. Manipulating Azobenzene Photoisomerization Through Strong Light-Molecule Coupling. *Nat. Commun.* **2018**, *9*, 4688.

https://dx.doi.org/10.1021/acs.jpclett.0c02399
J. Phys. Chem. Lett. 2020, 11, 9215−9223